

# XPS and FTIR Study of Silicon Oxynitride Thin Films

J. Viard,<sup>b</sup> E. Beche,<sup>c</sup> D. Perarnau,<sup>a</sup> R. Berjoan<sup>a</sup> and J. Durand<sup>b</sup>

<sup>a</sup>Institut de Science et de Génie des Matériaux et Procédés-UPR 8521 CNRS, BP 5 Odeillo-66120, Font-Romeu, France

<sup>b</sup>Laboratoire des Matériaux et Procédés Membranaires, UMR 5635 CNRS-UMII-ENSC, 8 Rue de l'École Normale, 34053 Montpellier Cédex, France

<sup>c</sup>Laboratoire d'Etudes et des Recherches sur les Matériaux et les Propriétés de Surface, Institut Polytechnique de Sévenans, 90010 Belfort, France

## Abstract

*SiN<sub>x</sub>, SiO<sub>x</sub> and SiO<sub>x</sub>H<sub>y</sub> deposits containing various hydrogen concentrations were prepared in a plasma enhanced chemical vapour deposition (PECVD) reactor using SiH<sub>4</sub>, NH<sub>3</sub> and N<sub>2</sub>O as precursor gases. These deposits were made for anti-reflection coatings on polymer substrates. In this work, we present a study of the compositions and the chemical environments of silicon, oxygen and nitrogen in these films by using XPS, XAES and FTIR characterization methods. It is shown that the SiO<sub>x</sub>N<sub>y</sub> deposits are constituted by various silicon environments which can be described by the presence of Si(O<sub>x</sub>N<sub>y</sub>H<sub>z</sub>) tetrahedra with  $x + y + z = 4$ . The amount of Si–H bonds increases in the deposits when the nitrogen concentration increases. Si–OH chemical bonds were detected for low nitrogen concentration. Published by Elsevier Science Limited.*

## 1 Introduction

SiO<sub>x</sub>N<sub>y</sub> thin films are widely known for their industrial applications in microelectronics and optics.<sup>1,2</sup> In this work, SiO<sub>x</sub>N<sub>y</sub>:H amorphous thin films were prepared by using a PECVD method, with the purpose of optical applications based on their various refractive index. A clear understanding of the nature of the chemical bonds in Si-based amorphous films is often difficult, due to the large variety of the chemical bonds which can be present. Here, we report the use of FTIR absorption bands associated with the use of XPS Si2p, 01s, N1s and XAES SiKL<sub>2,3</sub>L<sub>2,3</sub> transition to characterize the nature of the chemical bonds in SiO<sub>x</sub>N<sub>y</sub>:H films with varying nitrogen to oxygen ratios in these films.

## 2 Experimental Procedure

The SiO<sub>x</sub>N<sub>y</sub>:H deposits were prepared on Si wafers in an RF PECVD reactor<sup>3</sup> by using SiH<sub>4</sub>, NH<sub>3</sub> and

N<sub>2</sub>O as gaseous precursors. The SiH<sub>4</sub> flow rate was kept constant (SiH<sub>4</sub> = 2 sccm) and the ratio  $R = \text{NH}_3 / (\text{NH}_3 + \text{N}_2\text{O})$  was changed in the range  $0 \leq R \leq 1$ . The value of NH<sub>3</sub> + N<sub>2</sub>O was also kept constant at 20 sccm. Then, five SiO<sub>x</sub>N<sub>y</sub>:H deposits were analysed by XPS and FTIR spectroscopies.

The XPS measurements were carried out in a Cameca Riber Sia 250 device. The samples were first sputtered by an Argon ions beam accelerated under 3 keV. The ion current was near  $0.5 \mu\text{A cm}^{-2}$ . The photoelectron lines were shifted at lower kinetic energies by charging effects on the surfaces. Therefore, the peaks' positions were normalized by using the C1s peaks due to contamination carbon which was present on the as-deposited surface. For the energy normalization, we used also the Auger parameter  $\alpha'$  which is not sensitive to charging effects.<sup>4</sup> The changes of  $\alpha'$  values with the variations of compositions of the samples enable us to measure the true chemical shifts with an accuracy of about  $\pm 0.2 \text{ eV}$  of the peaks by using linear relations between the Si2p shifts or the SiKLL shifts and the  $\alpha'$  shifts. The XAES SiKL<sub>2,3</sub>L<sub>2,3</sub> Auger line was excited by the Bremsstrahlung X-rays from the Al anode. The vibrational spectra of the films were characterized with an FTIR Nicolet 4000. The absorption bands were measured by infra-red transmission through the deposit and the silicon substrate.

## 3 Results and Discussion

### 3.1 Deposits composition

The approximate atomic concentrations of silicon, oxygen and nitrogen were calculated from Si2p, 01s and N1s peaks areas measurements. For the semi-quantitative calculations of the concentrations of these last elements, we used sensitivity factors related to the ionization cross-sections

**Table 1.** Approximate composition of the  $\text{SiO}_x\text{N}_y\text{H}$  thin films resulting from the area measurements of Si2p, O1s and N1s XPS lines.

Deposit	R	Si	O	N
1	0	0.33	0.66	0
2	0.4	0.37	0.55	0.09
3	0.6	0.40	0.39	0.21
4	0.8	0.46	0.23	0.32
5	1.0	0.50	0	0.44

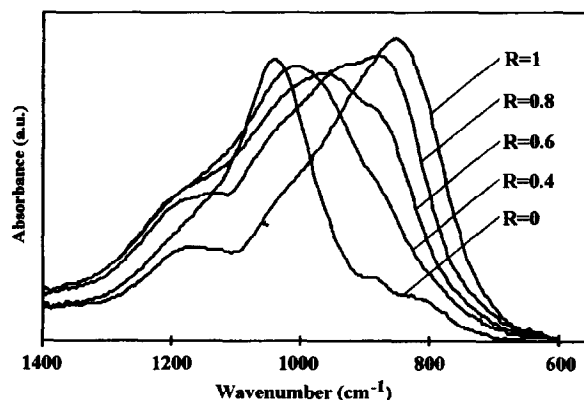
given by Scofield,<sup>5</sup> taking into account the transmission factor of the electron analyzer and the variations of the electron mean-free path with their kinetic energy.

Table 1 shows the variations of the Si, O and N compositions of the deposits on changing  $R$ . These compositions can be considered with a 10% relative accuracy.

For hydrogen, the atomic concentration of this element was assessed from the areas measurements of the Si-H and Si(OH-NH) infra-red absorption bands. The numbers of hydrogen atoms incorporated in the deposits were calculated by using a semi-quantitative method<sup>6-8</sup> based on the measurements of the absorption band areas  $A(\text{Si-H})$  and  $A(\text{O,N-H})$ .

From the results of these calculations, it was found that the atomic concentration of hydrogen increases with increasing  $R$ . This concentration was found in the range 5–10 at% for  $R=0$  and near 30 at% for  $R=1$ . Intermediate values of the hydrogen concentration near 30 at% calculated for the  $\text{SiN}_y\text{H}$  labelled 5 is often reported in previous works.<sup>9,10</sup>

From the results reported in Table 1, it is concluded that, for  $R=0$ , the deposit composition is similar to  $\text{SiO}_2$ , and, for  $R=1$ , the composition can be related to the presence of a hydrogenated amorphous  $\text{SiN}_y\text{H}$  layer containing Si-H bonds, as suggested by the detection of Si-H vibration and by an N/Si ratio  $\cong 0.9$ , lower than the N/Si ratio for  $\text{Si}_3\text{N}_4$  (1.33).

**Fig. 1.** FTIR absorption bands related to Si(O,N) stretching modes.

### 3.2 Si-H and Si-(O, H) absorption bands spectra

For samples 1 and 2, the Si-H stretching bands located around  $2240\text{ cm}^{-1}$  were very weak. These Si-H stretching bands were significantly broader for deposits 3, 4 and 5. The positions of these Si-H vibration bands were shifted at lower wave numbers when going from deposit 3 ( $\sim 2220\text{ cm}^{-1}$ ) to deposit 5 ( $\sim 2170\text{ cm}^{-1}$ ). This result indicates that the number of Si-H bonds increases when the value of the  $R$  ratio and the nitrogen concentration in the deposits increases.

Figure 1 shows the absorption bands attributed to Si-(O, N) stretching modes for all the samples examined in this work. This figure shows that the Si-(O, N) stretching bands are shifted to lower wave numbers for the nitrogen-rich samples 4 and 5. The shifts of the Si-(O, N) absorption bands can be attributed to an increase of the number of nitrogen atoms in the silicon tetrahedral environments.

### 3.3 XPS and XAES measurements

Table 2 summarizes the kinetic energies for SiKLL XAES transitions, the bonding energies of the photoelectron peaks Si2p, O1s and N1s, and the FWHM values measured for all these electron

**Table 2.** O1s, N1s, Si2p and SiKLL lines positions ( $E_B$ =binding energy,  $E_k$ =kinetic energy) and FWHM values for the deposits  $\text{SiO}_x\text{N}_y\text{H}$ 

Deposit	O1s		N1s		Si2p		SiKLL	
	$E_B$	FWHM	$E_B$	FWHM	$E_B$	FWHM	$E_k$	FWHM
1 ( $R=0$ )	532.21	2.4	—	—	103	2.5	1608.7	2.7
2 ( $R=0.4$ )	$\sim 533.5$	{3.9	397.5	2.4	103.9	{4.5	1607.6	5.6
	$\sim 532.2$				102.3			
3 ( $R=0.6$ )	532.4	2.8	398	2.5	102.4	3	1610.5	3.7
4 ( $R=0.8$ )	532.2	2.3	397.7	2.3	102	2.8	1611.5	3.1
5 ( $R=1$ )	532.1	2.5	397.8	2.2	101.6	2.5	1612.5	3.4

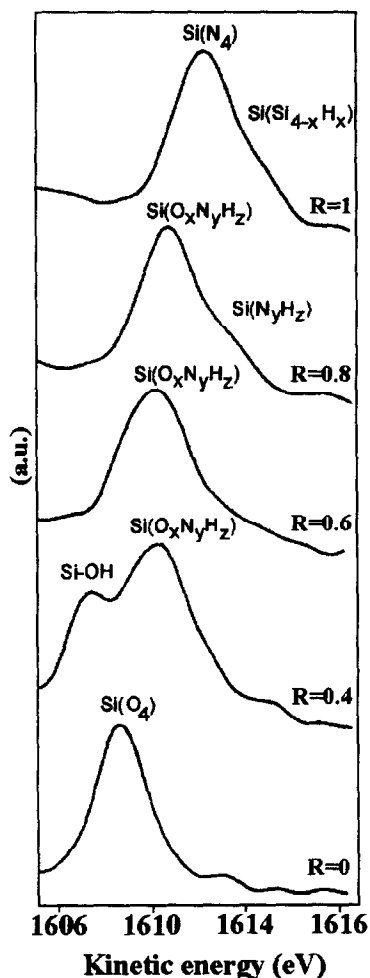


Fig. 2.  $\text{SiK}_{L_{2,3}}L_{2,3}$  auger lines excited by the Bremsstrahlung X-rays for  $\text{SiO}_x\text{N}_y\text{H}_z$  deposits.

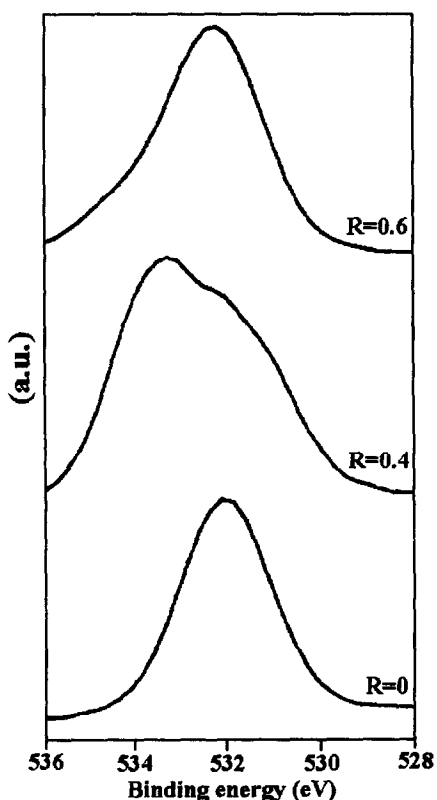
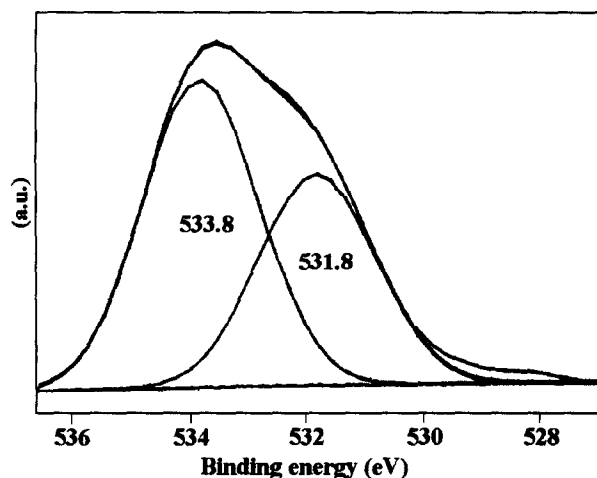
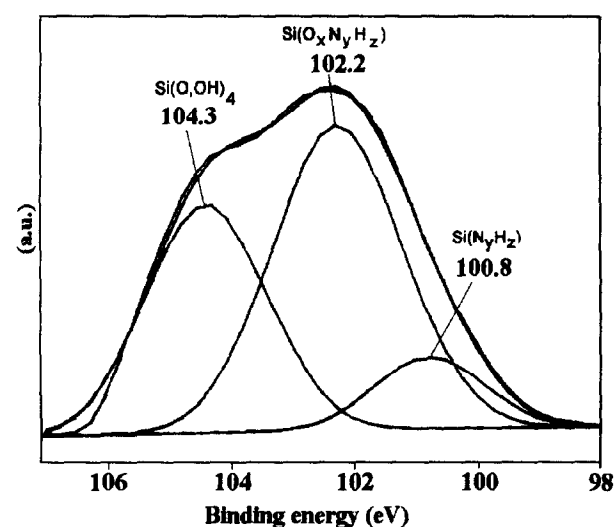


Fig. 3.  $01s$  photoelectron lines obtained for the deposits 1, 2 and 3.



(a)



(b)

Fig. 4.  $01s$  and  $\text{Si}2p$  peak fitting for the experimental peaks collected for deposit 2.

peaks. The results reported in Table 2 allow to conclude that the position of the  $\text{N}1s$  peak, and the full width at half maximum (FWHM) values of this peak, do not change with the nature and composition of the deposit ( $E_B \approx 397.7 \pm 0.3 \text{ eV}$  and  $\text{FWHM} \approx 2.3 \pm 0.2 \text{ eV}$ ). Inversely, broadening and splitting of  $01s$ ,  $\text{Si}2p$  and  $\text{SiKLL}$  are observed, and are particularly clear for samples 2 and 3. The position of the  $\text{Si}2p$  and  $\text{SiKLL}$  lines varies, respectively, from 103 to 101.6 eV and 1608.7 to 1612.5 eV. These values are characteristic of silicon nitrides (101.6 and 1612.5 eV)<sup>11,12</sup> and silica (103 and 1608.7 eV).<sup>11</sup>

Figure 2 shows the  $\text{SiKLL}$  features obtained for all the samples. The  $\text{SiKLL}$  feature for sample 1 is characteristic of an  $\text{SiO}_2$  film with the peak centered at 1608.7 eV. The  $\text{SiKLL}$  collected for sample 5 is the signature of an  $\text{SiN}_x\text{H}$  film with a peak centered at 1612.5 eV, and a shoulder between 1615 and 1616 eV which can be attributed to Si-Si and/or Si-H bonds. The KLL structure for sample 2 can be attributed to the presence of  $\text{Si}(\text{O}_x\text{N}_y\text{H}_z)$

tetrahedra at 1611.5 eV and  $\text{Si}(\text{N}_y\text{H}_z)$  for the shoulder located in the range 1613–1616 eV. The SiKLL line shape for sample 3 centered at 1610.5 eV can be attributed to  $\text{Si}(\text{O}_x\text{N}_y\text{H}_z)$  tetrahedra. For sample 2, the splitting of the SiKLL peak is probably due to the presence of numerous Si–OH bonds related to the presence of a second peak at 1607.6 eV. By comparing the 01s peaks for samples 1, 2 and 3 (Fig. 3), the presence of OH in deposit 2 seems to be confirmed by the broadening and splitting of the 01s peak. Figure 4 shows the 01s and Si2p peaks collected for sample 2. These peaks fittings show clearly the presence of two oxygen which are attributed to Si–O at 531.8 eV and Si–OH at 533.8 eV because the shifts observed between  $\text{O}^{2-}$  and  $\text{OH}^-$  are usually in the range 1.5–2 eV.<sup>4,13</sup> The three components extracted from the decomposition of the Si2p peak were attributed, respectively, at Si(O and/or OH) (104.3 eV),  $\text{Si}(\text{O}_x\text{N}_y\text{H}_z)$  bonds at 102.2 eV and  $\text{Si}(\text{N}_y\text{H}_z)$  at 100.8 eV. The presence of Si–Si bonds cannot be excluded.

#### 4 Conclusion

The preparation of  $\text{SiO}_x\text{N}_y\text{:H}$  deposits using the PECVD method described above and  $\text{SiH}_4$ ,  $\text{NH}_3$  and  $\text{N}_2\text{O}$  as precursors leads to the formation of many silicon tetrahedral bonds.

For  $R$  lower than 0.4, nitrogen was found with a small atomic concentration in the deposit.

For  $R=4$ , a large amount of OH bonds seems to be present.

For  $R>0.4$ , large amounts of nitrogen are incorporated in the films.

For  $R=0.6$ , the films appeared as constituted by  $\text{Si}(\text{O}_x\text{N}_y\text{H}_z)$  polysubstituted tetrahedra.

For  $0.8 \leq R \leq 1$ , the XAES SiKLL transitions allowed to distinguish  $\text{Si}(\text{O}_x\text{N}_y\text{H}_z)$  or  $\text{Si}(\text{N}_4)$  tetrahedra from  $\text{Si}(\text{N}_y\text{H}_z)$  or  $\text{Si}(\text{Si}_x\text{H}_{4-x})$  tetrahedra. For the high values of  $R$ , the hydrogen atoms are probably bonded essentially to nitrogen or silicon.

#### References

1. Finster, J., Klinkenberg, E. D., Heeg, J. and Braun, W., *Vacuum*, 1990, **41**, 1586.
2. Al-Jumaily, G. A., Mooney, T. A., Spungeon, W. A. and Dauplaise, H. M., *J. Vac. Sci. Technol.*, 1989, **A7**, 2280.
3. Viard, J., Thèse Doctorat, Université Montpellier II, 1996.
4. Briggs, D. and Seah, M. P., *Practical Surface Analysis*. J. Wiley and Sons Ltd, Chichester, UK, 1983.
5. Scofield, J. H., *J. Electron Spectrosc.*, 1976, **8**, 129.
6. Tsu, D. V. and Lucousky, G., *Journal of the Vacuum Science Technology*, 1986, **A4**(3), 480.
7. Adams, C. A., Alexander, F. B., Capio, C. D. and Smith, T. E., *Journal of the Electrochemical Society*, 1981, **126**(7), 1545.
8. Lanford, W. A. and Rand, M. J., *Journal of Applied Physics*, 1978, **49**(4), 2473.
9. Smith, D. I., Alimonda, A. S., Chau-Chen, C., Ready, S. E. and Wacker, B., *Journal of the Electrochemical Society*, 1990, **137**(2), 614.
10. Nguyen, S. V., Dobuzinsky, D., Dopp, D., Gleason, R., Gibson, M. and Fridman, S., *Thin Solid Films*, 1990, **194**, 595.
11. Wagner, C. D., Passoja, D. E., Hillery, H. F., Kimisky, J. G., Six, H. A., Jansen, W. T. and Taylor, J. A., *J. Vac. Sci. Technol.*, 1982, **21**, 933.
12. Wang, P. S., Malghan, S. G., Hsu, S. M. and Wittberg, T. N., *Surf. Interface Anal.*, 1994, **21**, 155.
13. Wagner, C. D., Riggs, W. M., Davis, L. E. and Moulder, J. F., *Handbook of X-Ray Photoelectron Spectroscopy*, ed. G. E. Muilenberg. Perkin-Elmer Corporation, Eden Prairie, MN.